Intrinsic structural distortion in orthorhombic perovskite oxides

J.-S. Zhou and J. B. Goodenough
Texas Materials Institute, University of Texas, Austin, Texas 78712, USA
(Received 16 February 2008; published 14 April 2008)

Octahedra in the orthorhombic perovskite structure are not rigid. The bond-length splitting at an octahedral site can be described by two degenerate vibration modes, the orthorhombic Q_2 and the tetragonal Q_3. A polar plot of $r=\rho=(Q_2^2+Q_2^2)^{1/2}$ and $\phi=\tan^{-1}(Q_3/Q_2)$ has been made to map out the site distortion as a function of the rare-earth ionic size for three families, $R\mathrm{FeO_3}$, $R\mathrm{VO_3}$, and $R\mathrm{MnO_3}$. The octahedral-site distortion deduced from $R\mathrm{FeO_3}$ is found to be intrinsic to orthorhombic perovskites and to strongly bias orbital ordering and spin ordering in compounds that have the same structure.

DOI: 10.1103/PhysRevB.77.132104 PACS number(s): 61.50.Ah, 61.50.Ks, 61.66.Fn, 64.70.K−

The perovskite oxides $AB\mathrm{O_3}$ have been intensively investigated due to a broad range of technical applications and complex physical properties that challenge the condensed-matter theory in a structure common to materials in the Earth's lower mantle. In a perovskite structure, 23 tilting systems can develop as a consequence of the geometric tolerance factor $t\equiv(A\text{-O})/[\sqrt{2}(B\text{-O})]<1$, where $(A\text{-O})$ and $(B\text{-O})$ are equilibrium bond lengths.[1–3] $\mathrm{GdFeO_3}$ becomes a prototype for the structural distortion in perovskites with the *Pbnm* space group, which is the most common perovskite structure. The $\mathrm{GdFeO_3}$-type distortion that is commonly cited refers to a cooperative octahedral-site rotation around the [110] and [001] axes of the cubic unit cell, which can also be described by the tilting system $a^-a^-b^+$ in the Glazer notation. As illustrated in Fig. 1, this cooperative octahedral-site rotation leads not only to the orthorhombic lattice parameters $b>a>c/\sqrt{2}$ but also to a bending of the *B*-O-*B* bond angle to $\theta=180°-\omega$. The orbital overlap integral over the *B*-O-*B* bonding array is therefore reduced by a factor of $\cos\theta$. This scenario can qualitatively explain the reduction in the Néel temperature T_N as θ decreases from 180° in an antiferromagnetic orthorhombic perovskite $RM\mathrm{O_3}$, where *R* is a rare earth and *M* is a transition metal. The cooperative octahedral-site rotation and corresponding shift of R^{3+} relative to its position in a cubic perovskite have been treated as primary parameters in calculations of the electronic structure[4] and the competition between different orbital ordering phases in cases wherein the *M* cation is Jahn-Teller active.[5] However, whereas the angle θ continuously increases with increasing ionic radius of the rare-earth ion (IR), the evolution of magnetic or orbital ordering phases as a function of IR always behaves anomalously at intermediate values of IR, as illustrated, for example, in $R\mathrm{TiO_3}$,[6] $R\mathrm{VO_3}$,[7] and $R\mathrm{MnO_3}$.[8] The structural distortions in the *Pbnm* perovskite are clearly more than those induced by octahedral-site tilting. Although it has been realized for a long time that the octahedra in the orthorhombic perovskites are not rigid[9] and the octahedral-site distortion is important in determining the electronic state,[10] a complete description of how they are distorted and whether there is a common rule for these octahedral-site distortions remain lacking. We have previously demonstrated,[11] by using the software SPUDS,[12] that the O-*M*-O bond angle in an octahedron starts to reduce from 90° universally at IR≈1.11 Å with increasing IR for the orthorhombic $RM\mathrm{O_3}$ perovskites given that the $\langle M\text{-O}\rangle$ bond length is about 2.0 Å. In this Brief Report, we will show an evolution, which was deduced from $R\mathrm{FeO_3}$ data, of the three Fe-O bond lengths at the octahedral site as a function of IR and will demonstrate that it is intrinsic to the orthorhombic perovskites. We will also demonstrate the close relationship between the evolutions of octahedral-site distortions and spin and orbital ordering temperatures as a function of IR.

Data from the classic crystallographic work by Marezio and co-workers[13,14] are redrawn in Fig. 2 together with the refinement results of high-energy x-ray powder diffraction for several members of the $R\mathrm{FeO_3}$ family.[15–17] Although it is a Jahn-Teller inactive system, the octahedral-site distortion is clearly visible beyond error bars of the bond-length data. As illustrated in Fig. 2, the three Fe-O bonds, Fe-$\mathrm{O_{21}}$ and Fe-$\mathrm{O_{22}}$ located in the basal plane and Fe-$\mathrm{O_1}$ along the *c* axis, split as IR decreases. The splitting peaks out near IR=1.11 Å, the

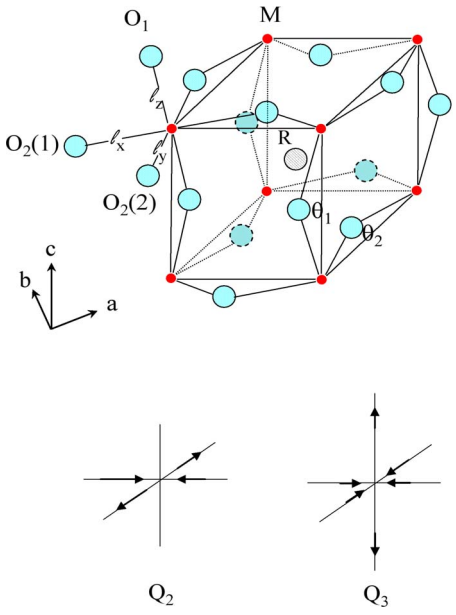

FIG. 1. (Color online) Schematic of the basic unit in the cell of the orthorhombic perovskite structure. The bond lengths 1_x, 1_y, and 1_z are defined in an octahedron for calculating the octahedral-site distortion modes. The arrows indicate the major axes of the orthorhombic cell. The lower part shows the octahedral-site distortion modes Q_2 and Q_3.

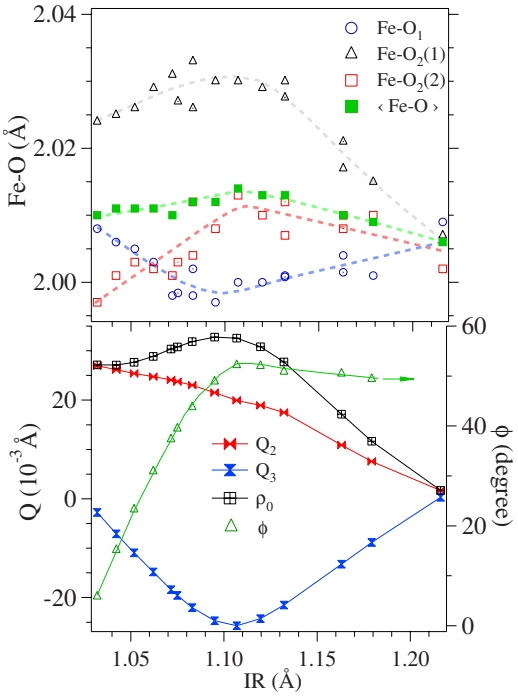

FIG. 2. (Color online) The upper panel: IR dependence of three Fe-O bond lengths in the orthorhombic RFeO$_3$. The structural data are from references. The dashed lines are a guide for the eyes. Curve fittings of these data were used to calculate $Q_2=\ell_x-\ell_y$, $Q_3=(2\ell_z-\ell_x-\ell_y)/\sqrt{3}$, $\rho=(Q_2^2+Q_3^2)^{1/2}$, and $\phi=\tan^{-1}(Q_3/Q_2)$, which are shown in the lower panel as a function of IR.

same place where the reduction from 90° of the O-M-O bond angle sets in as IR increases.[11] The bond-length splitting can be described by the displacements ℓ of the vibration modes $Q_2=\ell_x-\ell_y$ and $Q_3=(2\ell_z-\ell_x-\ell_y)/\sqrt{3}$, which are illustrated in the lower panel of Fig. 1. In order to explicitly demonstrate the evolution of the octahedral-site distortion as a function of IR, we have created a polar plot in Fig. 3 of $\rho=(Q_2^2+Q_3^2)^{1/2}$, the magnitude of the octahedral-site distortion versus the angle $\phi=\tan^{-1}(Q_3/Q_2)$, which opens from the Q_2 axis in an anticlockwise direction. For each RFeO$_3$ compound, there are two spots in this polar plot corresponding to a cooperative octahedral-site distortion on the two neighboring Fe^{3+} sites in a (001) plane. Along a circle with a given ρ in this plot, the octahedron with one long and two equal short bonds appears three times, but the long axis rotates in a different direction, i.e., at 0° (it is along the z axis), at 120° (along the x axis), and at 240° (along the y axis). The Fe-O bonds split into long, medium, and short bonds at an angle ϕ other than these three angles and these angles plus 180°. For the whole RFeO$_3$ family, the long bond is located in the basal plane and is alternately directed along directions close to the x and y axes, respectively. We focus on the site with the long bond close to the x axis and highlight the important features in the evolution of the room-temperature site distortion as a function of IR. (a) The total site distortion as measured by ρ nearly vanishes for the member with the largest IR in the family. (b) ρ increases along a line near 150° as IR decreases until IR$\approx$IR$_{Gd}$. (c) ρ starts to decrease along with a progressively reduced angle ϕ as IR decreases from IR$\approx$IR$_{Gd}$. The question left is whether the evolution of the octahedral-site distortions as a function of IR is intrinsic to the *Pbnm* perovskite. The room-temperature structural data[18–23] for RVO$_3$, in which orbitals remain disordered, are plotted in Fig. 3 in the same way as for RFeO$_3$. The two plots are comparable even quantitatively for most rare-earth atoms R. As far as we know, the structural work for the RTiO$_3$ family is not complete. However, the recent work of single-crystal diffraction on RTiO$_3$ (R=La, Nd, Sm, Gd, and Y) (Ref. 6) shows that the evolution of the Ti-O bond length as a function of IR is similar to that of RFeO$_3$, which is shown in Fig. 2. The comparison of the three families of perovskite RMO$_3$ leads us to conclude that the octahedral-site distortions are not random and system dependent but are intrinsic to the *Pbnm* perovskite structure.

In order to check whether this intrinsic site distortion biases the physical properties of the orthorhombic perovskites with the *Pbnm* space group, we bring in three examples:

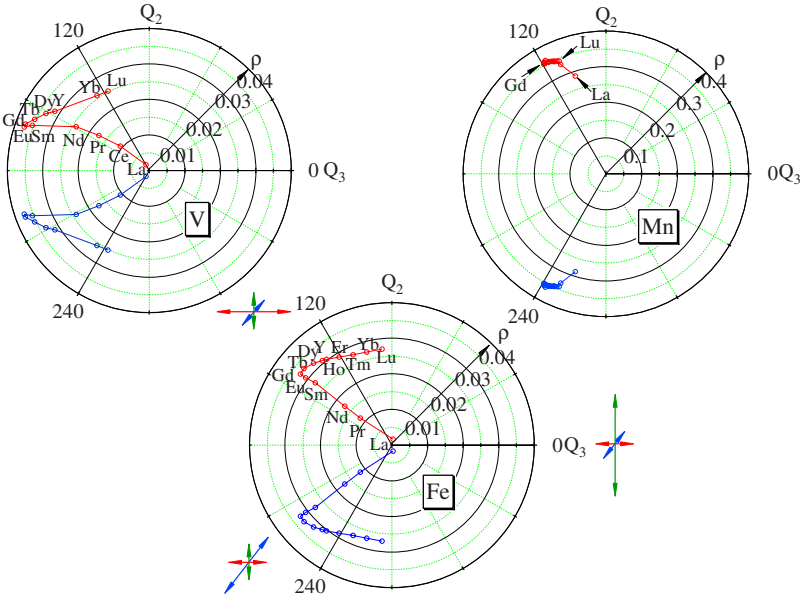

FIG. 3. (Color online) The polar plot of ρ and ϕ for three families of orthorhombic perovskites RMO$_3$ (M=V, Mn, and Fe). Most of the structural data of RVO$_3$ were from neutron diffraction (Refs. 15–20). The structural data for the RVO$_3$ (R=Pr, Sm, Eu, Gd, and Dy) were obtained by refining the powder diffraction from a Philips X'pert diffractometer. The data source for RMnO$_3$ can be found in Ref. 22. The three drawings surrounding the polar plot for RFeO$_3$ show the site distortion on a given circle ρ_0 along the directions of 0°, 120°, and 240°.

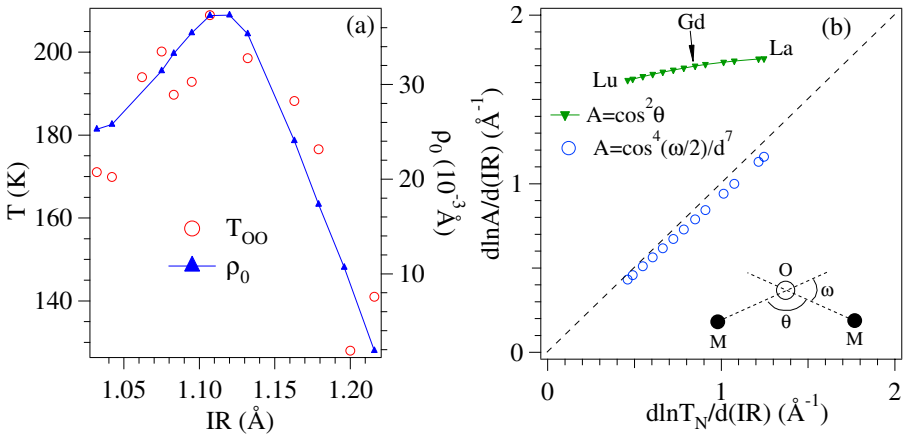

FIG. 4. (Color online) (a) The IR dependences of the orbital ordering temperature T_{OO} and the octahedral-site distortion ρ_0 for the RVO_3 family. (b) Plot of $d \ln A/d(\mathrm{IR})$ versus $d \ln T_N/d(\mathrm{IR})$ for $R\mathrm{FeO}_3$. The function A is defined inside the plot. The derivatives were made based on the curve fitting of A versus IR and T_N versus IR. The structural data that were used to calculate the function A are from Refs. 13–17 and a set of T_N is from Ref. 27. The inset shows the definition of angles θ and ω in a M-O-M bond.

orbital and/or spin ordering in the $R\mathrm{MnO}_3$ and RVO_3 families and spin ordering in $R\mathrm{FeO}_3$. We have made the same polar plot for $R\mathrm{MnO}_3$, wherein Mn^{3+} is Jahn-Teller active and the orbitals are ordered at room temperature. The bond-length data were previously published.[8] A cooperative Jahn-Teller ordering would make the occupied e orbital either $3z^2-r^2$ for all Mn^{3+} sites or $3x^2-r^2$ and $3y^2-r^2$ orbitals on alternating Mn sites. Since the intrinsic distortion allows the longest bond and a short bond located within the ab plane, $R\mathrm{MnO}_3$ prefers the latter orbital ordering. The orbital occupation significantly enlarges the long bond length relative to two equal short bonds in an octahedron. Therefore, we expect to see two spots on a large circle of ρ along the directions of 120° and 240°, which cover all members of the $R\mathrm{MnO}_3$ family. As shown in Fig. 3, data points representing the site distortion observed for $R\mathrm{MnO}_3$ do concentrate into two small areas near 120° and 240° on the circle with an $r=\langle\rho\rangle$ that is about an order of magnitude larger than $\rho_{\max}$ in $R\mathrm{FeO}_3$ and RVO_3. More importantly, the structural bias effect transforms the predicted single spot into a La-Gd-Lu triangle that resembles the one found in $R\mathrm{FeO}_3$, a birthmark for the orthorhombic perovskite structure. The possible structural bias effect on the Jahn-Teller distortion was first pointed out by Kanamori[24] when he found that two spots in (Q_2, Q_3) space for LaMnO_3 are slightly moved toward the Q_2 axis from 120° and 240°. Our complete demonstration of the cooperative Jahn-Teller distortion biased by the intrinsic structural distortion is made possible by the availability of systematic structural studies on the perovskite $R\mathrm{MnO}_3$ in recent years.

The relatively weaker orbital-lattice interaction for the t orbital system of the RVO_3 family than that for the e orbital in the $R\mathrm{MnO}_3$ family significantly lowers the orbital ordering temperature from $T_{JT} \geq 750$ K in $R\mathrm{MnO}_3$ to $T_{OO} \sim 200$ K in RVO_3. The dome-shaped curve of T_{OO} versus IR shown in Fig. 4(a) appears to have little to do with the V-O-V bond angle, which increases monotonically with IR. However, as shown by the curve of ρ_0 versus IR superimposed in the same plot, the two curves of T_{OO} versus IR and ρ_0 versus IR match each other surprisingly well. This observation clearly indicates the structural bias effect on the orbital ordering temperature in the perovskites RVO_3.

Where the M^{3+} ion is Jahn-Teller active, the intrinsic octahedral-site distortion has a more profound influence on physical properties than simply biasing the cooperative orbital ordering. We showed elsewhere[8] that the evolution of the Jahn-Teller energy versus IR, which is strongly biased by the intrinsic distortion, is responsible for a spin-ordering transition from type A to type E in the $R\mathrm{MnO}_3$ family. For the G-type orbital ordering below T_{OO} of RVO_3, the bias effect alters the degree of hybridization of the t^2 and te configurations in the ${}^3T_{1g}$ ground state of the V^{3+} ion.[25] In the $R\mathrm{TiO}_3$ family, the intrinsic octahedral-site distortion is correlated with the change in orbital ordering and the transition of magnetic ordering state from the antiferromagnetic phase to the ferromagnetic phase at an intermediate IR as IR decreases.[6] Even in a Jahn-Teller inactive system, the $\langle M\text{-O}\rangle$ bond modulation as a function of IR influences the spin-spin interaction. Through the following numerical test, we will show that the octahedral-site rotation alone is insufficient to account for the change in T_N as a function of IR in orthorhombic $R\mathrm{FeO}_3$.

The dependence of the superexchange interaction on the Fe-O-Fe bond angle was first postulated by Treves *et al.*[26] when a systematic Mössbauer measurement of the Néel temperature[27] and some preliminary structural data became available to them. They found that T_N monotonically increases as a function of $\langle\cos\theta\rangle = (\cos\theta_1 + 2\cos\theta_2)/3$. Under the assumption that the IR dependence of $\langle\text{Fe-O}\rangle$ is negligible, Boekema *et al.*[28] calculated the spin-spin coupling J for the superexchange interaction over the Fe-O-Fe array to be proportional to $\langle\cos^2\theta\rangle$ instead of $\langle\cos\theta\rangle$. Indeed, the curve of T_N versus $\langle\cos^2\theta\rangle$ is much more linear than that of T_N versus $\langle\cos\theta\rangle$. However, a linear relationship is not sufficient to justify an overlap integral $b^{\mathrm{cac}} \sim \cos\theta$ in the superexchange formula $T_N \sim (b^{\mathrm{cac}})^2/U$. A correct formula for the overlap integral b^{cac} as a function of the bond angle and bond length should make all data points lie along a 45° line through the origin in the plot of $d \ln[(b^{\mathrm{cac}})^2]/d(\mathrm{IR})$ versus $d \ln T_N/d(\mathrm{IR})$. As shown in Fig. 4(b), the plot with the func-

tion $b^{cac} \sim \cos\theta$ that was used by Boekema *et al.*[28] is not on the 45° line and is even not linear. Instead of suspecting the formula for the superexchange interaction, we believe that the octahedral-site distortion should also play some role. As shown in Fig. 2, ⟨Fe-O⟩ is not IR independent; it becomes slightly longer at intermediate values of IR. In order to check whether this small modulation in the ⟨Fe-O⟩ bond length versus IR is responsible for a nonlinear curve in the plot of $d \ln[(b^{cac})^2]/d(\mathrm{IR})$ versus $d \ln T_N/d(\mathrm{IR})$, we have included the contribution of ⟨Fe-O⟩ by using the formula $b \sim \cos^2(\omega/2)/d^{3.5}$ that was introduced by Harrison,[29] where d denotes the M-O bond length. It should be noted here that a $b \sim \cos(\omega/2)/d^{3.5}$ in Harrison's book[29] is for the M-O bond. Applying Harrison's formula[29] in the case of a $(180° - \omega)$ M-O-M bond gives $b \sim \cos^2(\omega/2)/d^{3.5}$. The plot of $d \ln A/d(\mathrm{IR})$ versus $d \ln T_N/d(\mathrm{IR})$ for $A = b^2 = \cos^4(\omega/2)/d^7$ indeed gives a nearly straight 45° line, which proves the importance of how local distortions influence T_N and the essential validity of how the M-O bond length enters the formula.

In conclusion, a comparative study between three $R\mathrm{MO_3}$ families (M=V, Mn, and Fe) and some members in the $R\mathrm{TiO_3}$ family with the orthorhombic perovskite structure reveals that the IR decrease not only causes a cooperative octahedral-site rotation but also induces an octahedral-site distortion. As shown in the polar plot (ρ, ϕ), the evolution of the octahedral-site distortion as a function of IR in these systems exhibits a common feature: the site distortion reaches its maximum at an intermediate IR. This intrinsic structural distortion biases the orbital and spin ordering in these systems. In the perovskite $R\mathrm{VO_3}$ family, the profile of the orbital ordering temperature T_{OO} as a function of IR well matches that of the site distortion measured by ρ_0 versus IR. In the perovskites $R\mathrm{FeO_3}$, the change in the overlap integral due to the octahedral rotation plays a dominant role in determining the Néel temperature T_N. However, T_N can only be precisely predicted by using the formula of the superexchange interaction if the bond-length modulation and bond angle enter the overlap integral as $b \sim \cos^2(\omega/2)/d^{3.5}$ in the case of a $(180° - \omega)$ M-O-M bond in perovskite oxides.

We thank the Robert A. Welch Foundation and the NSF for financial support.

[1] A. M. Glazer, Acta Crystallogr., Sect. B: Struct. Crystallogr. Cryst. Chem. **28**, 3384 (1972).
[2] P. M. Woodward, Acta Crystallogr., Sect. B: Struct. Sci. **53**, 32 (1997); **53**, 44 (1997).
[3] K. S. Aleksandrov and J. Bartolome, Phase Transition **74**, 255 (2001).
[4] T. Mizokawa and A. Fujimori, Phys. Rev. B **54**, 5368 (1996).
[5] T. Mizokawa, D. I. Khomskii, and G. A. Sawatzky, Phys. Rev. B **60**, 7309 (1999).
[6] A. C. Komarek, H. Roth, M. Cwik, W.-D. Stein, J. Baier, M. Kriener, F. Bouree, T. Lorenz, and M. Braden, Phys. Rev. B **75**, 224402 (2007).
[7] S. Miyasaka, Y. Okimoto, M. Iwama, and Y. Tokura, Phys. Rev. B **68**, 100406(R) (2003).
[8] J.-S. Zhou and J. B. Goodenough, Phys. Rev. Lett. **96**, 247202 (2006).
[9] M. O'Keeffe and B. G. Hyde, Acta Crystallogr., Sect. B: Struct. Crystallogr. Cryst. Chem. **33**, 3802 (1977).
[10] I. V. Solovyev, Phys. Rev. B **74**, 054412 (2006).
[11] J.-S. Zhou and J. B. Goodenough, Phys. Rev. Lett. **94**, 065501 (2005).
[12] M. W. Lufaso and P. M. Woodward, Acta Crystallogr., Sect. B: Struct. Sci. **57**, 725 (2001).
[13] M. Marezio and P. D. Dernier, Mater. Res. Bull. **6**, 23 (1971).
[14] M. Marezio, J. P. Remeika, and P. D. Dernier, Acta Crystallogr., Sect. B: Struct. Crystallogr. Cryst. Chem. **26**, 2008 (1970).
[15] D. Du Boulay, E. N. Maslen, V. A. Streltsov, and N. Ishizawa, Acta Crystallogr., Sect. B: Struct. Sci. **51**, 921 (1995).
[16] E. N. Maslen, V. A. Streltsov, and N. Ishizawa, Acta Crystallogr., Sect. B: Struct. Sci. **52**, 406 (1996).
[17] V. A. Streltsov and N. Ishizawa, Acta Crystallogr., Sect. A: Found. Crystallogr. **55**, 1 (1999).
[18] P. Bordet, C. Chaillout, M. Marezio, Q. Huang, A. Santoro, S.-W. Cheong, H. Takagi, C. S. Oglesby, and B. Batlogg, J. Solid State Chem. **106**, 253 (1993).
[19] A. Munoz, J. A. Alonso, M. T. Casais, M. J. Martinez-Lope, J. L. Martinez, and M. T. Fernandez-Diaz, Phys. Rev. B **68**, 144429 (2003).
[20] M. Reehuis, C. Ulrich, P. Pattison, B. Ouladdiaf, M. C. Rheinstadter, M. Ohl, L. P. Regnault, M. Miyasaka, Y. Tokura, and B. Keimer, Phys. Rev. B **73**, 094440 (2006).
[21] G. R. Blake, T. T. M. Palstra, Y. Ren, A. A. Nugroho, and A. A. Menovsky, Phys. Rev. B **65**, 174112 (2002).
[22] A. Munoz, J. A. Alonso, M. T. Casais, M. J. Martinez-Lope, J. L Martinez, and M. T. Fernandez-Diaz, J. Mater. Chem. **13**, 1234 (2003).
[23] A. Munoz, J. A. Alonso, M. T. Casais, M. J. Martinez-Lope, J. L Martinez, and M. T. Fernandez-Diaz, Chem. Mater. **16**, 1544 (2004).
[24] J. Kanamori, J. Appl. Phys. **31**, S14 (1960).
[25] J.-S. Zhou, J. B. Goodenough, J.-Q. Yan, and Y. Ren, Phys. Rev. Lett. **99**, 156401 (2007).
[26] D. Treves, M. Eibschutz, and P. Coppens, Phys. Lett. **18**, 216 (1965).
[27] M. Eibschutz, S. Shtrikman, and D. Treves, Phys. Rev. **156**, 562 (1967).
[28] C. Boekema, F. van der Woude, and G. A. Sawatzky, Int. J. Magn. **3**, 341 (1972).
[29] W. A. Harrison, *Electronic Structure and the Properties of Solids* (Dover, New York, 1989).